INTERNATIONAL JOURNAL FOR NUMERICAL METHODS IN FLUIDS, VOL. 21, 323–335 (1995)

ON IDENTIFICATION OF FLOW SEPARATION AND VORTICES IN INTERNAL PERIODIC FLOWS

MOSHE ROSENFELD

Department of Fluid Mechanics and Heat Transfer, Faculty of Engineering, Tel Aviv University, Tel Aviv 69978, Israel

SUMMARY

To permit simplified analysis of complex time-dependent flows, possible relationship between the near-wall flow, flow separation and vortices are studied numerically for a flow in a constricted two-dimensional channel. The pulsating incoming wave-form consists of a steady flow, followed by a half-sinus flow superimposed on the steady component. One pair of vortices is created in each cycle, one vortex near each wall. The vortices propagate downstream in the next cycles, promoting flow separation as they move. Existing flow separation criteria were not found to be uniformly valid. A relation between the near-wall flow and the vortical system exists only during the steady incoming flow phase of the cycle. It seems that local criteria of flow separation cannot be found for complex internal pulsating flow fields. However, the vorticity field can be utilized, even in complex time-periodic flows, for identifying vortices that have been formed by the roll-up of shear layers.

KEY WORDS: flow separation; time-periodic, unsteady; vortices; incompressible; Navier–Stokes

1. INTRODUCTION

The identification of flow separation and vortices in two-dimensional internal flows with a time-periodic flow at the entrance is studied. The identification of flow separation is important because it affects global properties as well as integral quantities such as pressure drop and heat and mass transfer rates. In steady two-dimensional flows the pattern of the streamlines uniquely defines the structure of the flow field, including the flow-spearated regions. The separation points coincide with the points where the skin friction (wall vorticity) vanishes. In unsteady flows it is impossible to relate uniquely flow-separated regions with the instantaneous streamlines.[1] For example, numerous experimental and numerical evidences show that the vanishing of the wall vorticity does not coincide with the separation point.[2–4]

It is widely accepted that the separation point (in both steady and unsteady flows) is the point where the flow ceases to follow the contour of the body and breaks away from the wall.[3,5] This intuitive definition is based on many flow visualizations but is difficult to quantify or to relate to the instantaneous state of the flow. Experimental works may use dye flow visualization techniques to determine flow separation in unsteady flows.[5] In numerical simulations the streaklines yield similar information. However, the calculation of the streaklines of unsteady flows require large computational resources. To simplify the recognition process, simpler methods were sought, yielding several criteria for identifying flow separation; see details in Section 4.1. The criteria were developed for external boundary-layer-like flows. In the present work, however, internal flows are considered. In many internal flows a thin boundary layer does not exist. On the contrary, large flow-separated regions, which may develop into vortices, are formed in many cases.[6–10] Moreover, most existing unsteady

CCC 0271–2091/95/040323–13
© 1995 by John Wiley & Sons, Ltd.
Received April 1994
Revised January 1995

separation criteria have been proposed for flows which are not periodic in time. This raises questions about the validity of existing separation criteria for internal periodic flows. The applicability of these critera to a class of internal time-periodic flows will be investigated in Section 4.2.

The relationship between the near-wall flow and the vortical (separated) flow away from the wall was studied extensively for steady and external three-dimensional flows.[11] The existence of a correlation between the near-wall flow and the outer flow may offer many advantages in the study of complex time-dependent vortical flows because of the simplicity and data reduction gained by the elimination of one physical dimension (the transverse dimension). An attempt is made in Section 5 to correlate the near-wall flow with the global flow field for internal time-periodic flows.

One of the distinctive properties of pulsating internal flows is their strong dependence on governing factors such as the geometry or the Strouhal and Reynolds numbers.[10] Therefore the problem of periodic separation cannot be studied in general terms. In the present study we test existing separation criteria and the possible correlation between the near-wall flow and the 'outer' flow for the example of a pulsating flow imposed at the entrance of an asymmetric constricted two-dimensional channel. The pulsating flow in non-uniform channels was found in many works to result in flow separation[6,7] and the development of multiple vortices,[8,9] which in some cases propagated downstream.[10,12] Our interest is focused less on the identification of separation points and more on the identification of flow separation and formation of vortical flows.

2. METHODOLOGY

2.1. *Formulation*

The geometrical set-up is shown in Figure 1(a); it is similar to that used in the experiments of Park.[12] The channel is composed of two straight parallel plates at a distance h from each other (length units are scaled by h). On the upper wall a circular arc constriction is added with a constriction size $a/h = 0{\cdot}56$.

The equations governing the flow of a constant density isothermal incompressible fluid in a fixed control volume with face $\mathbf{S}$ and volume V are the conservation-of-mass equation

$$\oint_S d\mathbf{S} \cdot \mathbf{u} = 0 \tag{1}$$

and the Navier–Stokes equations

$$\frac{d}{dt}\int_V \mathbf{u}\, dV = \oint_S d\mathbf{S} \cdot \mathbf{T}, \tag{2a}$$

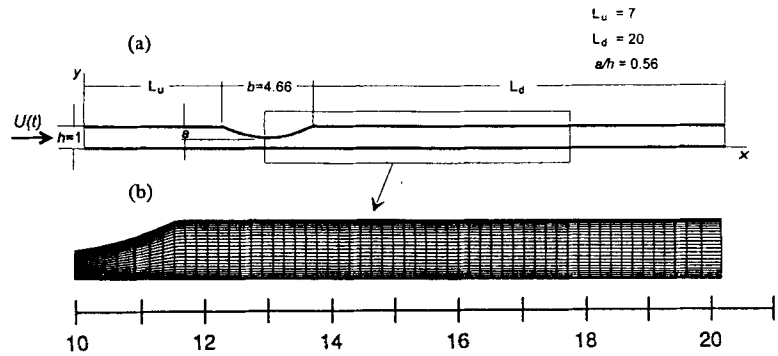

Figure 1. (a) Geometry of computational domain (not to scale) and (b) mesh in region downstream of constriction (only every fourth mesh point is shown)

where u is the velocity vector, t is the time, dV is a volume element and dS is the area element vector. For Newtonian fluids the tensor T is given by

$$\mathbf{T} = -\mathbf{uu} - P\mathbf{I} + \nu[\nabla\mathbf{u} + (\nabla\mathbf{u})^T], \tag{2b}$$

where $\mathbf{I}$ is the identify tensor, $\nabla\mathbf{u}$ is the gradient of $\mathbf{u}$ and $(\nabla\mathbf{u})^T$ is its transpose. The pressure is P and ν is the kinematic viscosity.

The wave-form of the average axial velocity ($U(t)$ at the entrance is defined for each cycle as in the experiments of Park:[12]

$$U(t) = \begin{cases} U_s, & 0 < t/T \leq \frac{1}{2}, \\ U_s - U_p \sin(2\pi t/T), & \frac{1}{2} < t/T \leq 1, \end{cases} \tag{3}$$

where T is the period and U_s and U_p are the steady and oscillating components respectively. In the present study $U_s = 1$ and $U_p = 1{\cdot}217$, yielding a mean velocity U_m=1·387. The start of each cycle corresponds to $t/T = 0$, i.e. t/T is the phase of the cycle (not the absolute time). We shall refer to a phase inside a cycle also according to the variation in the incoming flow. Thus the steady incoming flow phase refers to the first half of the cycle, $\frac{1}{2} \geq t/T \geq 0$, while the acceleration and deceleration phases refer to $\frac{3}{4} \geq t/T > \frac{1}{2}$ and $1 > t/T > \frac{3}{4}$ respectively.

At the upstream boundary a fully developed flow is specified for the wave-form (3). At the downstream boundary, Neumann boundary conditions are given for the velocity components: $\partial\mathbf{u}/\partial x = 0$, where x is the streamwise Cartesian co-ordinate. On the upper and lower walls, no-slip and no-injection conditions are specified: $\mathrm{u} = 0$.

The Reynolds and Strouhal numbers, defined by $Re = U_m h/\nu$ and $St = h/U_m T$ respectively, are $Re = 182$ and $St = 0{\cdot}368$. These values (as well as U_s and U_p) duplicate the 'base case' defined in the experiments of Park.[12]

2.2. *Numerical method*

The laminar unsteady incompressible Navier–Stokes equations with primitive variables are solved via a solution procedure developed by Rosenfeld *et al.*[13] and Rosenfeld and Kwak.[14,15] The formation of the governing equations, the discretization procedure and the numerical solution stages are combined to yield an accurate and efficient solution method for complex time-dependent flows in generalized co-ordinate systems. The governing equations, written in the integral form (1) and (2), are discretized by finite volumes. The scheme is second-order-accurate in space and time. The discrete equations are solved by a fractional step method with an approximate factorization of the momentum equations. The convergence rate of the Poisson equation is accelerated by a multigrid procedure. The interested reader may find the details of the method in the reference cited above.

2.3. *Mesh and numerical details*

A transfinite algebraic mesh generator was employed with 289 × 97 points in the axial and transverse directions respectively. The finest resolution in the axial direction is specified downstream of the constriction, where the flow field is most complex. A blow-up of the mesh in this region is shown in Figure 1(b); for clarity, only every *fourth* mesh point is shown in each direction.

The solution was started from a fully developed parabolic velocity profile and was marched in time until a (graphically accurate) time-periodic flow was attained in the entire region of interest. The results to be presented are for the 11th cycle from the start of the solution. By this time a steady time-periodic flow is established, so that all the results refer to the periodic solution. The numerical method itself was validated for a series of internal and external flow problems.[12,13]

The geometry, the incoming wave-form and the Reynolds and Strouhal numbers were chosen to be identical with the 'base case' considered in the experiments of Park.[12] The reason is that detailed comparisons with these experimental results were carried out by Rosenfeld.[16] The vortical flow field was accurately captured by the numerical simulations and very good agreement was obtained in the propagation speed of the vortices for a wide range of parameters. In addition, the numerical model and the calculated results were also extensively tested for numerical consistency and accuracy. It was shown that the mesh size and the number of time steps were adequate and that the location and type of boundary conditions were correctly chosen. The validated results permit the further investigation of the flow in detail not possible using the experiments only.

3. THE FLOW FIELD

The instantaneous streamlines are shown in Figure 2(a) for 10 equally spaced instances along one cycle. In the first half of the cycle a vortex is observed on the upper wall lee of the constriction, followed by a series of decaying vortices downstream. On the lower wall another series of vortices is observed. The whole system propagates downstream, resulting in a wavy core flow with decaying transverse oscillations. In the acceleration phase of the cycle ($\frac{3}{4} > t/T > \frac{1}{2}$) the vortices seem to diminish, the core streamlines straighten out and the flow in the diverting part of the constriction attaches to the walls. In the deceleration phase ($1 > t/T > \frac{3}{4}$) the vortex lee of the constriction reappears, along with the other vortices of the flow that seemed to disappear during the acceleration phase. In the steady phase of the incoming flow the upstream vortices expand and get stronger.

The pattern of the streamlines is useful in analysing steady flows, yet it might be misleading for usteady flows.[4,5] The large increase in the incoming flow velocity wrongly implied the disappearance of the vortices in the instantaneous streamline plots, as Figure 2(b) clearly exhibits. In this figure the

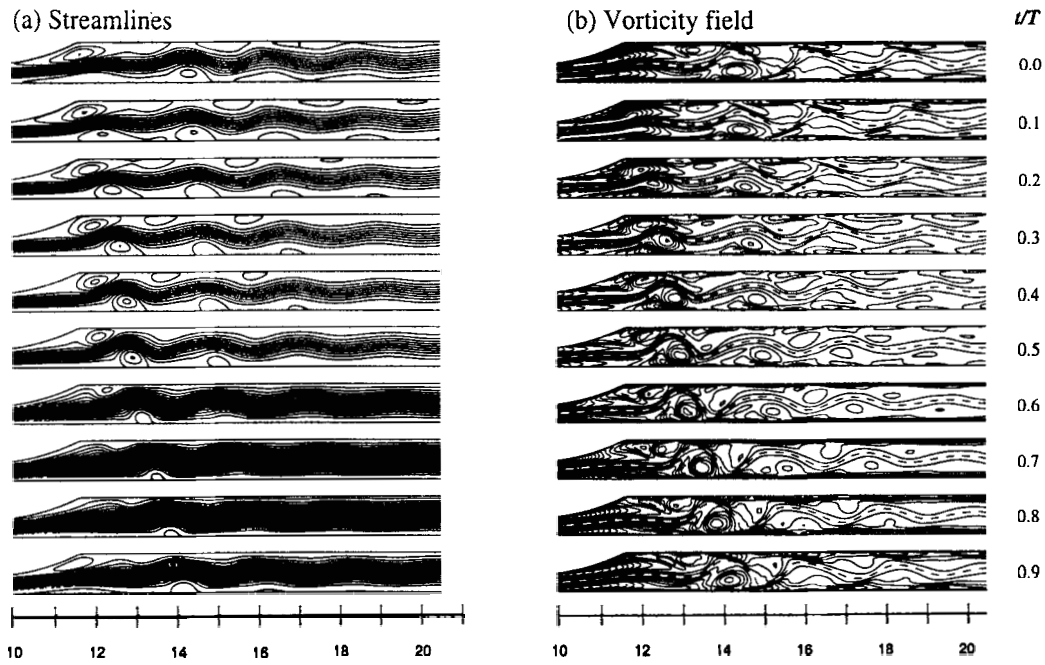

Figure 2. (a) Instantaneous streamlines and (b) vorticity field at 10 equally spaced instances of a cycle. The increment between the vorticity contour lines is 2·5. Zero values are shown by broken lines

vorticity field is given for the same 10 phases of the cycle. The transverse oscillations in the vorticity field remain fairly uniform over the entire cycle, in contrast with what was observed in the pattern of the streamlines. The difference is especially prominent in the acceleration phase of the flow, when the instantaneous streamlines are almost parallel to the walls, while the vorticity field exhibits large transverse variations. The streamlines also indicated the diminishing of the vortices in the acceleration phase and their reappearance in the deceleration phase. The vorticity field, however, reveals that the size and strength of the vortices hardly change.

A new pair of vortices is developed in each cycle, one vortex near each wall. In any instance, vortices generated at previous cycles still co-exist downstream, creating two trains of moving vortices near the walls and a wavy core flow between them. Following the notation of Park,[12] the upper and lower wall vortices are labelled by A and B respectively (Figure 2(a)). The co-existing vortices are differentiated by an index that refers to the formation cycle relative to the present cycle n. Thus B_{n-1} refers to the lower wall vortex that was generated in the previous cycle, etc.

The first pair of vortices is formed in the region $12{\cdot}5 > x > 11$ (the formation region). In the deceleration phase, vorticity is carried away from the walls through shear layers. Being far from the retarding forces of the walls, the shear layers roll up by $t/T = 0{\cdot}2$ and form the two vortices A_n and B_n; see Figure 2(b) (and Figure 3 below). The vorticity included in each vortex originates from the boundary layer far upstream from the location of the vortex itself. In the propagation region ($x > 12{\cdot}5$) the flow field is dominated by the propagating vortices. The vortices are advected downstream with a small propagation speed during the first half of the cycle. In the second half the propagation speed increases along with the growth of the incoming velocity. The flow in the propagation region resembles the flow due to the interaction between a boundary layer flow and a convected vortex filament in the outer region.[17] The moving vortices force the flow in the propagation region to separate from the walls. In the formation region, on the other hand, the flow separation is excited by the decelerating flow and the non-uniform geometry. Beneath the propagating vortices a counter-vorticity region is created by the swirling motion of the vortices. The wall is characterized by alternate regions of negative and positive vorticity that last over a large portion of the cycle; see also Section 5.

The streaklines at the same 10 phases of a cycle are shown in Figure 3. Vortices can be identified from the time sequence of the streaklines based on the definition of a vortex as a mass of fluid moving around a common (stationary or moving) axis.[1] The properties of the flow exhibited by the streaklines are similar to those described previously. The formation of the first pair of vortices is characterized by the rapid penetration of particles into the core flow and the roll-up of the vortices by $t/T > 0{\cdot}2$. After the formation of A_n and B_n they expand up to the beginning of the acceleration phase. During the acceleration their sizes remain approximately constant, while in the deceleration phase they deform into elongated vortices. In the next cycle A_{n-1} and B_{n-1} continue to deform and the vortical motion is clear only in the core of the vortices.

The similarity of the streaklines to the vorticity field in two-dimensional flows is of special interest. Many experimental works noticed the close agreement between the two.[5,18] The shape of the vortices and the location of their centres, as found from the vorticity field (Figure 2(b)) and the streaklines (Figure 3), are indeed identical in the steady incoming velocity phase of the pulsating case. A small deviation is found in the acceleration phase, but the discrepancy diminishes in the deceleration phase. This is in contrast with the instantaneous streamlines, which completely missed the details of the flow field in the second half of the cycle.

Obviously the streaklines are the most reliable technique for identifying flow separation in unsteady flows, especially if the flow is driven by large periodic components. However, the computational resources needed to calculate the streaklines might be beyond routine capabilities, especially for complex flows. In many cases the vorticity field may offer a cheap alternative for identifying vortices and associated flow-separated regions. Nevertheless, the vorticity field cannot be always related

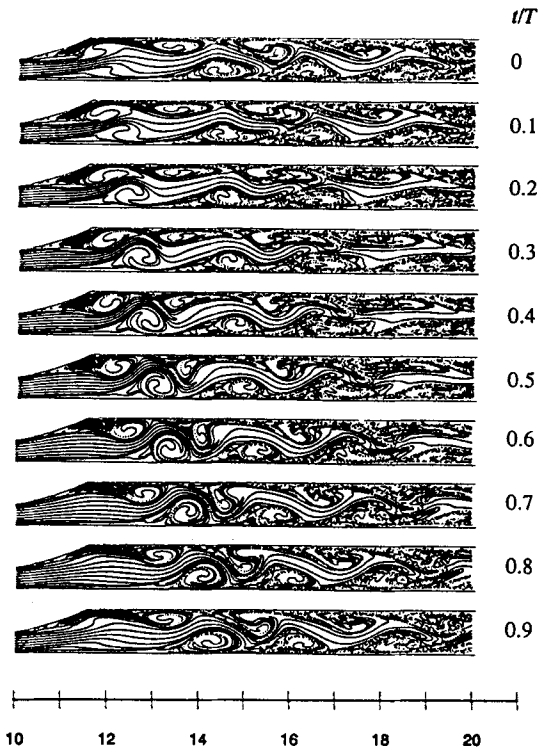

Figure 3. Streaklines at 10 equally spaced instances of a cycle

uniquely to flow separation, even in steady flows.[1] It can, however, reliably identify vortices that result from the roll-up of shear layers, by locating closed vorticity contour lines.

4. UNSTEADY FLOW SEPARATION

In the present section, unsteady flow separation criteria are evaluated for the class of internal flow problems that are of interest in the present study. Existing criteria are reviewed in Section 4.1, while in Section 4.2 the applicability of these criteria is studied. New recommendations are given in Section 4.3. The findings in the upper and lower walls are similar and therefore only the results of the lower wall are depicted.

4.1. Existing flow separation criteria

4.1.1. Unsteady flow separation criteria. The well-known MRS criterion (after Moore, Rott and Sears) defines the separation point in an unsteady flow as the point where both the shear stress and the velocity magnitude vanish in a co-ordinate system moving with the separation point. Another criterion was suggested by Wang,[19] who noticed the mathematical similarity between the unsteady two-dimensional boundary layer equations and the steady three-dimensional boundary layer equations. On the basis of his studies on the topology of the skin friction lines near three-dimensional steady flow separation,[20] Wang proposed for the case of unsteady two-dimensional flows to study the topology of the curves defined by

$$\frac{\mathrm{d}x}{\mathrm{d}t} = \left.\frac{\partial u}{\partial n}\right|_{\text{wall}} = -\omega_{\text{wall}}, \tag{4}$$

where n is the normal direction, ω_{wall} is the wall vorticity and u is the axial velocity component. The lines are called 'skin friction lines', in analogy with the three-dimensional case. Wang[19] identified unsteady separation with the envelope of the skin friction lines. He found that the flow separates if many skin friction lines converge into a single line, the convergence line, that describes the motion of the separation point in the x–t plane. Supporting evidences were found in several studies of flows with boundary layer character; see e.g. References 19 and 21.

These criteria of flow separation in unsteady cases might not be universal, because they are mainly based on experimental observations without rigorous theoretical basis. Didden and Ho[22] and Ho[23] concentrated on flow separation *symptoms* to overcome the lack of a universal criterion. They identified experimentally several symptoms for the case of a vortex-induced unsteady separation. The symptoms were thickening of the boundary layer, ejection of vorticity, zero shear stress, occurrence of a saddle point, initiation of a local shear layer and large transverse velocity. These symptoms indeed occur in many separated flows,[23] but they do not appear in a predefined order and so cannot be regarded as separation criteria.

4.1.2. Time-periodic flow separation criteria. Flow separation in time-periodic flows is even less well studied. In the case of oscillating boundary layer flows Despard and Miller[24] related the commencement of laminar boundary layer separation with the initial occurrence of zero velocity or reverse flow throughout the cycle. Supporting evidences were found by Koromilas and Telionis.[25] They mapped experimentally the velocity field over a backward-facing circular arc placed in a steady upstream flow with a 5% periodic disturbance superimposed on it. The oscillations in the velocity field were found to be magnified drastically as the separation point was approached. Similar findings were made by Mezaris *et al.*[26] for a pulsating boundary layer flow. They suggested using this observation as a separation criterion for time-periodic cases.

4.2. Evaluation of flow separation criteria

The validity of these flow separation criteria for the present problem will be evaluated in this subsection. We shall adopt the widely accepted definition of the separation point as the point where the streaklines break away from the wall.[3–5] This 'exact' separation point will be compared with the various separation criteria. The determination of the separation points using the streaklines might be inaccurate, because the breakaway point is determined visually. However, in many cases the breakaway is quite sudden, so that the inaccuracy introduced in this graphical definition is tolerable. Anyway, in the present study the exact location of the separation point is less important than the identification of the occurrence of flow separation.

To determine the separation points of the B-vortices, the streaklines were calculated for 20 *axial* locations near the lower wall. An example of the resulting streaklines is shown in Figure 4 for $t/T = 0{\cdot}5$. The breakaway that marks the formation of B_n (point L) is gradual, but it has a steeper slope away from the wall. The identification of the separation points of B_{n-1} and B_{n-2} (points M and N) is easier.

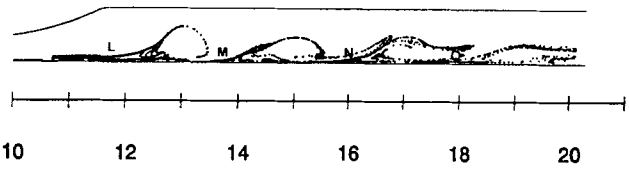

Figure 4. Streaklines released from vicinity of lower wall ($t/T = 05$)

4.2.1. Unsteady flow separation criteria. Figure 5 plots in the x–t plane the separation point lines (SPLs), the zero-vorticity lines (ZVLs) and the 'skin friction lines' (SFLs) on the lower wall. The SPL describes the motion of the separation point (as found from the streaklines). The ZVL is the line that joins the points of vanishing vorticity. In each case the four separate lines correspond to the four vortices that co-exist on the lower wall. The four SPLs can be determined for the entire cycle, while the ZVL disappears during the acceleration and part of the deceleration phases (except for B_n). The downstream propagation of the vortices is exhibited by the oblique lines in the x–t plane. In agreement with previous studies of unsteady flows, the SPL and the ZVL do not coincide.[2–4] The distance between them is almost constant ($1 \pm 0{\cdot}1$), indicating a similar propagation velocity. However, unlike in other studies, the separation points are always *upstream* of the zero-vorticity points.

The skin friction lines are calculated from equation (1). The integration is carried out for 40 equally spaced points along the x-direction. In addition, the SFL calculation is restarted at eight phases of the cycle. The resulting pattern of skin friction lines is indeed similar to that obtained for three-dimensional steady flows.[11,20] Four convergence lines are found in the first half of the cycle, corresponding to the four co-existing B-vortices. The skin friction lines merge from both sides, classifying the convergence lines as 'open separation' lines.[19–20] The convergence line of B_n (the most upstream convergence line) forms only after $t/T > 0{\cdot}2$. This correlates with the completion of the roll-up of B_n, supporting the conjecture of Wang that convergence lines coincide with separation lines. The convergence lines of the downstream vortices B_{n-1} and B_{n-2} form after $t/T > 0{\cdot}9$, in agreement with the reappearance of recirculating flow in the instantaneous streamlines (Figure 2(a)). In the acceleration phase, convergence lines do not form. The absence of convergence lines and ZVLs is a result of the increase in the magnitude of the wall vorticity in the acceleration phase of the incoming flow, eliminating zero values of the vorticity. However, the changes in the vorticity field away from the body are small and the vortices themselves are only slightly affected; see Section 3.

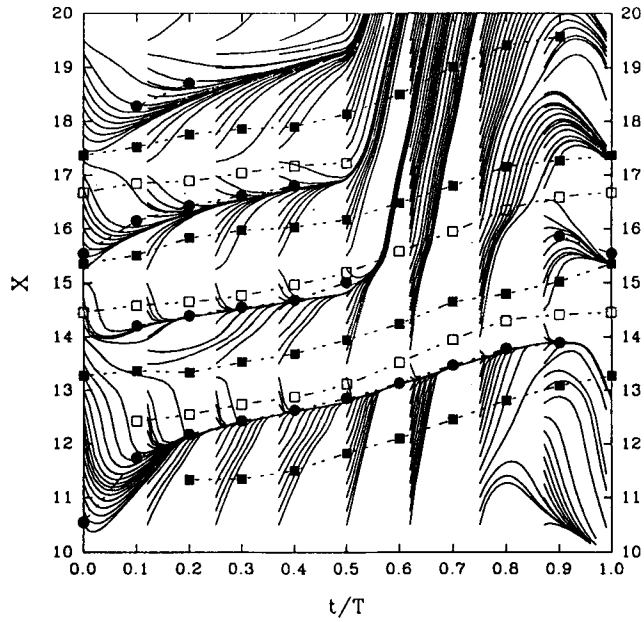

Figure 5. 'Skin friction' lines (———), separation point lines (—■—), zero-vorticity lines (—●—) and vortex centre lines (—□—) in x–t plane (lower wall)

In the boundary layer calculations of Wang[19,20] the vorticity always vanishes upstream of the separation line. In the present internal flow case the convergence lines coincide with the ZVLs and are *downstream* of the SPLs. The centres of the vortices, also shown in Figure 5, are always downstream of the convergence lines but at a relatively short distance from them.

The implementation of the MRS condition requires the knowledge of the separation point velocity to locate the stagnation points in a co-ordinate system moving with the separation point. Usually this velocity is unknown and therefore the implementation of the MRS condition is difficult. In the present case the velocity of the separation point can be calculated from the motion of the separation point. However, we have found no points in the flow field that satisfy the MRS condition. The inapplicability of the MRS condition for even external unsteady flow separation characterized by 'open separation' lines was also reported by Wang.[21] Doligalski and Walker[17] found as well that the MRS condition is not likely to be satisfied in the case of a boundary layer separating in response to the motion of a vortex (as in the case in the propagation region of the present case). Consequently, the inapplicability of the MRS criterion supports previous findings for similar flows.

Most of the separation symptoms listed by Didden and Ho[22] and Ho[23] can indeed by found in the present results. Zero shear stress is found near the separation points. A thick boundary layer and a larger transverse velocity precede the separation of the flow. However, the vorticity that feeds the first pair of vortices cannot be described as ejected from the walls as Didden and Ho[22] found, because the separation is a gradual process. Also, local shear layers are initiated by the moving vortices, as was mentioned in the list of separation symptoms. However, these shear layers include counter-velocity, which contributes to the destruction of the moving vortices.

4.2.2. Time-periodic flow separation criteria. The criterion of Despard and Miller[24] was also found to be inapplicable. The moving vortices and the large oscillating component of the incoming flow induce both upstream and downstream velocities at each point near the walls (depending on the phase of the cycle), excluding the existence of regions with reverse velocity over the entire cycle. Even in the inception region of vortex A, lee of the constriction, reverse flow during the entire cycle was not found.

To compare with the criterion of Mezaris *et al.*[26] for periodic flows, Figure 6 presents the amplitude of the first Fourier harmonic in a time decomposition of the axial velocity (u). The amplitude of the first harmonic of u, which is the most dominant oscillating component, exhibits an organized pattern in the propagation region. Several sets of oval-shaped contour lines appear near each wall, with the peaks in the centre of the closed lines.

In the formation region of the first pair of vortices the large increase in the fluctuating component is similar to that found by Mezaris *et al.*[26] In the propagation region an increase in the fluctuating components can be found in alternate regions along the wall. However, in Reference 26 the separation point oscillated with a small amplitude around a mean position. In the present case the vortices propagate monotonically downstream. It is not possible to relate the centre of the closed contour lines in the propagation region to the commencement of flow separation, because every point near the walls (downstream of the constriction) is evenually swept by the propagating vortices. Nevertheless, the similarity in the fluctuating components of these two very different flow problems is remarkable.

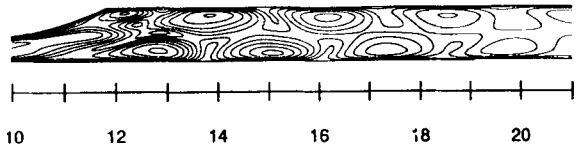

Figure 6. First Fourier harmonic of the axial velocity. The increment between contour lines is 0·2

4.3. General remarks and recommendations

In the steady incoming flow phase the convergence lines of the SFLs were able to identify the presence of flow separation, although the separation points do not coincide with the convergence lines. In the second half of the cycle, however, none of the separation criteria holds, even approximately. The reasons for the disagreement are obvious. Existing studies were performed for external flows that have a distinct boundary layer character. This is not true for the present internal flow case. The size of the separated region is of O(1) and a thin boundary layer flow does not precede the separation. The separation points in previous studies were nearly stationary, while in the present problem they move downstream monotonically. Moreover, the separated regions form closed vortices, whereas in most other studies the separation point precedes the formation of a wake flow. It is doubtful whether a simple criterion can be found at all for complex internal flows. The inevitable conclusion is that existing unsteady separation criteria cannot be simply extended to internal flows with large forced oscillating components.

To retain some hope, we have to recall the close resemblance found between the streaklines and the vorticity field, including in the region of the vortices (Section 3). Therefore the vorticity field is suggested as an alternative approach for identifying vortices in complex flows. Although this requires more processing effort than local criteria (which probably do not exist in complex flows), it is still easy to perform. However, even this complete field analysis does not apply to all cases, but only to vortical regions that have been generated by the *roll-up* of shear layers, i.e. closed vorticity contour lines are found.

5. NEAR-WALL FLOW

Section 4 discussed the absence of a uniformly valid correlation for internal pulsating flows between flow separation and the separation points, the zero-vorticity points or even the 'skin friction lines'. In the present section we investigate further the near-wall flow and its relationship with the flow away from the wall. If a unique relationship can be established, the investigation of similar flow fields might be significantly simplified, as is done for external three-dimensional steady flows.[11]

The close resemblance between the vorticity field and the streaklines might indicate that a relationship does exist between the wall vorticity and the propagating vortices in the 'outer' flow. Figure 7 plots the vorticity on the lower wall in the x-t plane. The full and dotted contour lines indicate positive and negative vorticity values respectively, while the broken contours are the zero, vorticity lines. The large variations in the incoming flow wave-form are exhibited in the pattern of the wall vorticity. Short-scale oscillations observed near the discontinuous parts of the time derivative of the incoming flow ($t/T = 0$ and $0{\cdot}5$) are due to the sudden change in the mass rate flow. In the steady upstream phase of the cycle the vorticity varies mainly along the streamwise direction. The variations with time are smaller and are mainly a result of the moving vortices. At the beginning of the acceleration phase the magnitude of the wall vorticity increases abruptly, leading to vertical contour lines near $t/T = 0{\cdot}5$.

In the second half of the cycle the vorticity variations with time are of the same order of magnitude as the variations along the x-direction, creating closed contour lines. In the acceleration phase the (negative) magnitude of the vorticity increases, while in the deceleration phase the magnitude decreases according to the variation in the incoming flow. However, the maximal wall vorticity is not found at $t/T = 0{\cdot}75$ when the inflow mass rate is maximal, but earlier at $t/T \approx 0{\cdot}64$–$0{\cdot}67$ (depending on the axial location), which is equivalent to a phase lead of about 35°.

The sign of the wall vorticity indicates the direction of the near-wall flow, while the points of vanishing vorticity coincide with stagnation points. Figure 7 shows that alternate regions of upstream

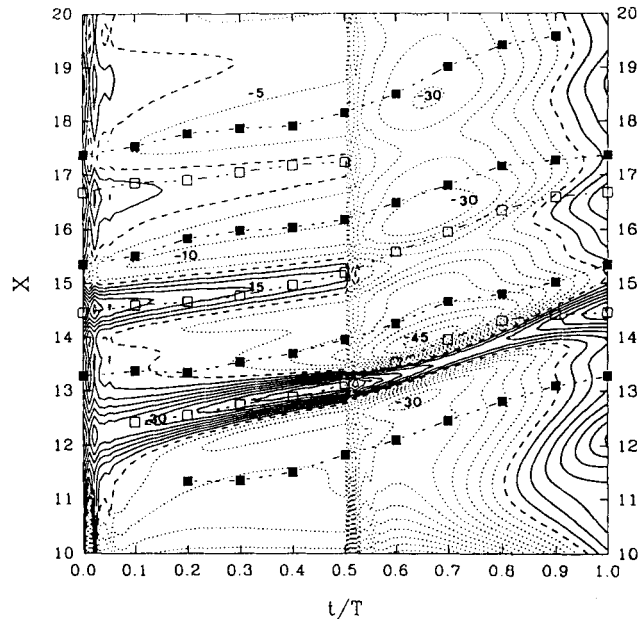

Figure 7. Vorticity on lower wall in x–t plane. The increment between contour lines is 5. Positive, negative and zero vorticities are shown by full, dotted and broken contour lines respectively. Separation point lines (—■—) and vortex centre lines (—□—) are also plotted

and downstream flow are found near the lower wall in the first half of the cycle. The regions of reverse flow are beneath the vortices, while downstream flow prevails between the moving vortices. In the acceleration phase the flow along the entire wall is downstream, except in a very small domain beneath B_n ($x \approx 13{\cdot}5$). However, this does not mean that the vortices are annihilated. The vorticity field, Figure 2(b), shows that the excess vorticity stays bound to the walls, generating a thin layer of high vorticity. This layer does not feed the vortices, maintaining the same system of vortices as in the steady incoming flow phase. Reverse flow regions are formed near the wall during the deceleration phase (note, however, that in unsteady flows a reverse flow does not necessarily indicate the presence of flow separation). In the steady incoming flow phase the regions of reverse flow near the wall diminish to the regions beneath the moving vortices.

An issue we raised is whether there is a relationship between the near-wall flow and the vortices away from the wall. To investigate this topic, the separation point lines and the centres of the B-vortices are also shown in Figure 7. In the steady incoming flow phase a relationship can indeed be found. The separation points lie in the regions of minimal vorticity (maximal negative value), while the centres of the vortices are located above the points where the wall vorticity is maximal. In the second half of the cycle a clear relation between the near-wall flow and the outer flow does not exist. Although the same trends are observed, the increase in the incoming flow changes the wall vorticity rapidly, whereas the vortices respond more slowly. Consequently, the separation and vortex centre points are located downstream of the respective minimum and maximum of the wall vorticity. The largest deviation occurs when the magnitude of the vorticity is maximal ($t/T \approx 0{\cdot}65$).

6. CONCLUDING REMARKS

The identification of flow separation and separation points as well as the relation between the near-wall flow and the outer vortical flow were investigated in the present paper for an internal pulsating flow. In

the steady incoming flow phase the criterion of Wang[19] predicted reasonably well the separation of the flow. However, most other separation criteria failed. Similarly, in the steady phase of the cycle a unique relationship could be found between the near-wall flow and the 'outer' vortical flow. However, in the second half of the cycle, which included variations of order $O(1)$ in the incoming flow, none of the separation criteria was found to be applicable and no relation could be found between the near-wall flow and the outer flow.

The streaklines can visualize accurately flow separation and vortices in unsteady flows. Besides the streaklines, the vorticity field is probably the most reliable visualization technique for complex unsteady flows. The vorticity field closely follows the pattern of the streaklines in the vortical regions during the entire cycle. Therefore we recommend it for identifying vortices that form through the roll-up of shear layers.

Other pulsating and internal flow cases may behave differently and the present study does not claim to be valid for all possible cases. The study should be repeated for other classes of pulsatile vortical flows to extend the generality of the results. However, we believe that similar results hold for cases that are dominated by large moving vortices. This belief is supported by a series of (unreported) flow simulations that we have conducted for a wide range of governing parameters.

REFERENCES

1. H. J. Lugt, 'The dilemma of defining a vortex', in U. Muller *et al.* (eds), *Recent Developments in Theoretical and Experimental Fluid Mechanics—Compressible and Incompressible Flows*, Springer, New York, 1979.
2. D. P. Telionis, 'Review—unsteady boundary layers, separated and attached', *J. Fluids Eng.*, **101**, 29–43 (1979).
3. D. P. Telionis, in *Springer Series in Computational Physics, Unsteady Viscous Flows*, Springer, New York, 1981, pp. 279–282.
4. T. Sarpkaya, 'Brief reviews of some time-dependent flows', *ASME J. Fluids Eng.*, 114, 283–298 (1992).
5. S. Taneda, 'Visual study of unsteady separated flows around bodies', *Prog. Aerospace Sci.*, **17**, 287–348 (1977).
6. B. F. Armaly, F. J. Durst, C. F. Pereira and B. Schonung, 'Experimental and theoretical investigation of backward-facing step flow', *J. Fluid Mech.*, 127, 473–496 (1983).
7. I. J. Sobey, 'Observation of waves during oscillatory channel flow', *J. Fluid Mech.*, **151**, 395–426 (1985).
8. O. R. Tutty, 'Pulsatile flow in a constricted channel', *J. Biomech. Eng.*, 114, 50–54 (1992).
9. O. R. Tutty and T. J. Pedley, 'Pulsatile flow in a constricted channel', *J. Fluid Mech.*, **247**, 179–204 (1993).
10. M. Rosenfeld, 'A numerical study of incompressible laminar pulsating flow behind a constriction', *J. Fluid. Mech.*, accepted
11. W. Tobak and D. J. Peak, 'Topology of three-dimensional separated flows', *Ann. Rev. Fluid Mech.*, 14, 61–85 (1982).
12. D. K. Park, 'A biofluid mechanics study of arterial stenoses', *M.Sc. Thesis*, Lehigh University, Bethlehem, PA, 1989.
13. M. Rosenfeld, D. Kwak and M. Vinokur, 'A fractional-step solution method for the unsteady incompressible Navier–Stokes equations in generalized coordinate systems', *J. Comput. Phys.*, **94**, 102–137 (1991).
14. M. Rosenfeld and D. Kwak, 'Time-dependent solutions for viscous incompressible flows in moving coordinates', *Int. j. numer. methods fluids*, 13, 1311–1328 (1991).
15. M. Rosenfeld and D. Kwak, 'Multi-grid acceleration of fractional step solvers of incompressible Navier–Stokes equations in generalized curvilinear coordinate systems', *AIAA J.*, **31**, 1792–1800 (1993).
16. M. Rosenfeld, 'Validation of numerical simulation of incompressible pulsatile flow in a constricted channel', *Comput. Fluids*, 22, 139–156 (1993).
17. T. L. Doligalski and J. D. A. Walker, 'The boundary layer induced by a convected two-dimensional vortex', *J. Fluid Mech.*, **139**, 1–28 (1984).
18. R. A. Petersen and R. C. Clough, 'The influence of higher harmonics on vortex pairing in an axisymmetric mixing layer', *J. Fluid Mech.*, 239, 81–98 (1992).
19. K. C. Wang, 'Unsteady boundary layer separation', *Martin Marietta Report MML TR 79-16C*, 1979.
20. K. C. Wang, 'Boundary layer over a blunt body at high incident with an open-type separation', *Proc. R. Soc. Lond. A*, **340**, 33–55, (1974).
21. K. W. Wang, 'On current controversy about unsteady separation', in T. Cebeci (ed.), *Numerical and Physical Aspects of Aerodynamic Flows*, Springer, New York, 1982, Chap. 1.
22. N. Didden and C. M. Ho, 'Unsteady separation in a boundary layer produced by an impinging jet', *J. Fluid Mech.*, 160, 135–256 (1985).
23. C. H. Ho, 'An alternative look at the unsteady separation phenomenon', in A. Krothapalli and C. A. Smith (eds), *Recent Advances in Aerodynamics*, Springer, New York, 1986, pp. 165–178.

24. R. A. Despard and J. A. Miller, 'Separation in oscillating laminar boundary-layer flows', *J. Fluid Mech.*, **47**, 21–31 (1971).
25. C.A. Koromilas and D. P. Telionis, 'Unsteady laminar separation: an experimental study', *J. Fluid Mech.*, 97, 347–384 (1980).
26. T. B. Mezaris, C. Barbi, G. S. Jones and D. P. Telionis, 'Separation and wake of pulsating laminar flow', *Philos. Trans. R. Soc. Lond. A*, **322**, 493–523 (1987).